Development of Nanocomposites of Bentonite with Polyaniline and Poly(methacrylic acid)

Rahul Singhal, Monika Datta

Department of Chemistry, University of Delhi, Delhi 110007, India

Received 17 April 2006; accepted 1 August 2006
DOI 10.1002/app.25334
Published online in Wiley InterScience (www.interscience.wiley.com).

ABSTRACT: Nanocomposites of bentonite with polyaniline (PANI), poly(methacrylic acid) (PMAA), and poly (aniline-*co*-methacrylic acid) (PANI-*co*-PMAA) were prepared by *in situ* intercalative polymerization technique. The nanocomposites were characterized by FTIR and UV–visible spectroscopies, XRD, SEM, TEM, as well as TG-DTA studies. The *in situ* intercalative polymerization of PANI, PMAA, and PANI-*co*-PMAA within bentonite layers was confirmed by FTIR, XRD, SEM, as well as TEM studies. XRD confirmed the intercalation of polymers and copolymer in bentonite. The average particle size of the nanocomposites was found to be in the range of 250–500 nm. The thermal stability was found be the highest for PANI-*co*-PMAA-bentonite. The swelling behavior studies suggest that these nanocomposites hold potential for their utilization in absorption of toxic materials from waste water. © 2006 Wiley Periodicals, Inc. J Appl Polym Sci 103: 3299–3306, 2007

Key words: bentonite; polyaniline; nanocomposite; poly (methacrylic acid); intercalation; swelling studies

INTRODUCTION

Polymer nanocomposites containing layered structures have attracted much attention during the past few decades owing to their unique structures and intriguing properties, which have led to their increased application in various fields.[1] Among all the potential nanocomposite precursors, those based on clay and layered silicates have been extensively investigated because the polymer chains can be easily intercalated between the silicate layers.[1,2] The nanometer-size particles of these nanocomposites exhibit markedly improved mechanical, thermal, optical, and physicochemical properties when compared with the pure polymer or conventional (microscale) composites. Kojima and coworkers[3] were the first to demonstrate this for nylon–clay nanocomposites. Since then, several strategies have been considered to prepare polymer-layered silicate nanocomposites. They are exfoliation–adsorption,[4–8] *in situ* intercalative polymerization,[9–11]melt intercalation,[12–14] and template synthesis.[15,16]

Recently, montmorillonite (MMT), a layered material with lamellar structure, has attracted the researchers' interest for the preparation of polymer/clay nanocomposites because of its higher surface area, high aspect ratio, improved adhesion between polymer and particle, and lower amount of loading required to achieve remarkable properties.[17] Many MMT nanocomposites have been investigated, for instance, poly(ε-caprolactone)/MMT,[18] epoxy/MMT,[19] PU/MMT,[20] PVA/MMT,[21] PP/MMT,[22] and PS/MMT.[23] The polymer/clay nanocomposites are prepared either by blending the clay with the polymers or by *in situ* polymerization of the monomers or prepolymers. The dispersion of nanolayers of the organophilic clay is found to boost the thermal stability, mechanical strength, molecular barrier as well as flame retardant properties of the polymers.[20]

Among many conducting polymers, polyaniline (PANI) is a promising material for commercial applications of conducting polymers because of environmental stability, easy processing, and economic efficiency.[24,25] Kim and coworkers[26] reported PANI–montmorillonite composites with intercalated nanostructures. Wu et al.[27] synthesized nanocomposites of PANI-Na^+MMT using an emulsion polymerization process using DBSA as an emulsifier. Yang and Chen[28] have also reported the preparation of nanocomposites of PANI with organically modified clays. Lately, Yoshimoto et al.[29] adopted an ecofriendly mechanochemical intercalation technique for the synthesis of PANI-MMT nanocomposites which was found to exhibit higher intercalation of anilium ions than by conventional solution method.

Literature survey reveals that only a few authors have investigated the nanocomposites of bentonite.[30] Forte et al.[31] used ^{13}C solid-state NMR for the determination of the structure of clay/methyl methacrylate copolymer nanocomposites. They prepared interlayer complexes of several MMA/2-(*N*-methyl

Correspondence to: M. Datta (monikadatta@yahoo.co.in).

Journal of Applied Polymer Science, Vol. 103, 3299–3306 (2007)

N,*N*-diethylammonium iodide) ethyl acrylate (MDEA) copolymers with two different clays (bentonite and hectorite) using two different preparations, and then complexes were studied in the clay layer and, more important, on the average distances between clay layers. Given the relatively high content of paramagnetic centers in bentonite, which is ~ 50 times more paramagnetic than hectorite, the SPE/MAS and CP/MAS spectra of the different nanocomposites with bentonite show differences according to the proximity of the different copolymer moieties to the clay surface. Some investigations on the synthesis of bentonite/polyacrylamide[32] nanocomposites have also been reported; however, literature survey reveals that no work has been reported on the synthesis of bentonite nanocomposites with PANI or PMAA.

The present work reports the synthesis of nanocomposites of bentonite with PANI, PMAA, and poly (aniline-*co*-methacrylic acid) using *in situ* intercalative polymerization. The nanocomposites were further characterized by FTIR, UV–visible, TG-DTA, SEM, as well as TEM studies. The absorption and swelling/deswelling behavior were investigated.

EXPERIMENTAL

Bentonite clay was procured from Aldrich (Chemical Co., USA) and was used as such. Aniline (Sigma–Aldrich) was distilled twice under reduced pressure prior to use. Sodium chloride (Sigma–Aldrich), ammonium persulphate (Sigma–Aldrich), *N*-acetyl *N*,*N*,*N*-trimethyl ammonium bromide (CTAB) (Sigma–Adlrich), methacrylic acid (Sigma–Aldrich), and HCl (Merck, India) were used as such without further purification.

Preparation of Na^+-bentonite

Bentonite clay (5 g), air dried at 80°C, was suspended in 100 mL of distilled water and allowed to stand overnight. The clay was filtered and 35 mL of 1.0*M* aqueous NaCl solution was added to it with slow continuous stirring at room temperature (25°C). It was then left undisturbed for 24 h to ensure maximum exchange of ions present in the day by Na^+ ions in the solution. The clay suspension was centrifuged and the mother liquor was decanted. The procedure was repeated twice to have maximum exchange ions. The clay was then recovered by centrifugation after washing the suspension with double-distilled water to ensure complete removal of chloride ions. This was done by testing the filtrate with silver nitrate solution. The clay so obtained was in sodium form.

Modification of Na^+-bentonite clay

Bentonite was organically modified with an alkyl ammonium salt before it was intercalated with the monomer. Bentonite (5 g) was suspended and stirred for 2 h in 200 mL distilled water. The suspension was then heated to 60°C and an aqueous solution of CTAB (0.5 g/100 mL) was gradually added with continuous stirring for 1 h. The organically exchanged bentonite was then centrifuged and washed several times with distilled water till no bromide ions were detected. The CTAB-bentonite clay was then dried in a vacuum oven at 60°C for 72 h.[2]

Synthesis of PANI-bentonite nanocomposite

A measured volume of freshly distilled aniline (3 mL) was syringed slowly into a well stirred suspension containing bentonite (~ 1 g). Ammonium persulphate (0.2 g) was added, followed by the addition of 40 mL of 1*N* HCl at 20°C. The gradual change of color from light gray to green was indicative of the formation of PANI. After 3 h, the total mass was centrifuged and washed several times with distilled water and methanol. The nanocomposite thus obtained was dried under vacuum at 60°C for 24 h, to obtain an intense dark green powder. Following the same procedure PMAA-bentonite as well as PANI-*co*-PMAA-bentonite nanocomposites were prepared and were designated as PMAA-bentonite and PANI-*co*-PMAA-bentonite respectively. The PMAA-bentonite was obtained as an intense yellow powder while PANI-*co*-PMAA-bentonite synthesized was light green in color.

Characterization

FTIR spectra of the nanocomposites were taken on a PerkinElmer FTIR spectrophotometer in KBr between 4000 to 400 cm^{-1}. UV–visible spectra were taken on PerkinElmer lambda EZ-221. TEM was recorded on Morgagni 268-D TEM (FEI, Netherlands). Scanning electron micrographs were taken on JEOL JSM840 scanning electron microscope. X-ray diffractograms were recorded on X-ray diffractometer (model Philips PW3710) using Cu Kα radiations. TG-DTA was recorded on a 2960 SDT V3.0F at a heating rate of 5°C/min and a flow rate of 100 mL/min, after annealing the samples for 24 h at 100°C. For swelling studies accurately weighed 0.5 g dry pellet (150–250 μm thick) of different bentonite samples was immersed in 1 L of distilled water. The swollen pellet was taken out at different times and filtered through a 100-mesh nylon gauze and weighed. Similar procedure was adopted for the study of 10% xylene absorption and 10% toluene absorption. The

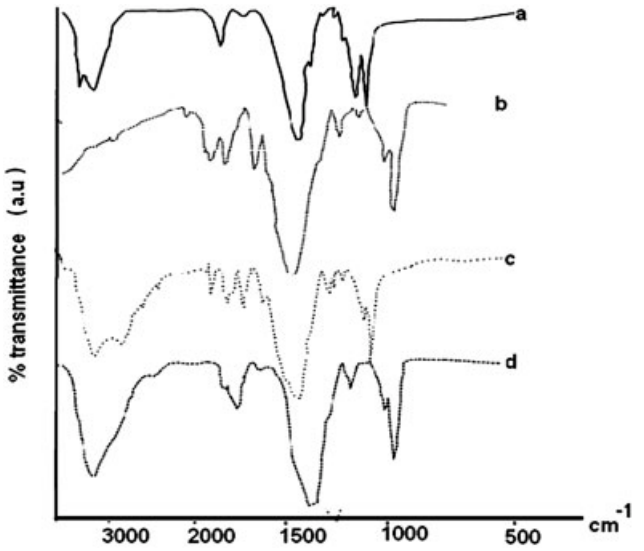

Figure 1 FTIR spectra of (a) bentonite,(b) PANI/bentonite, (c)PMAA/Bentonite, and (d)PANI-*co*-PMAA/bentonite.

absorbency at time t (Q_t) was calculated using the following equation:

$$\frac{W_t - W_0}{W_0} \quad (1)$$

where W_t is the weight of the swollen pellet at a certain time, and W_0 is the weight of the dry one. Swelling capacity was measured after absorbing for 5 h.[4]

RESULTS AND DISCUSSION

FTIR spectra

FTIT spectra of bentonite, PANI-bentonite and PANI-*co*-PMAA-bentonite are shown in Figure 1. The pristine bentonite spectra [Fig. 1(a)] shows characteristic peaks of lattice water stretching vibrations υ (O—H) at 3418 cm^{-1}, CH_2 asymmetric stretching vibrations υ (C—H) at 2953 cm^{-1}, H—O—H bending δ (H—O—H) at 1634 cm^{-1}, υ (Si—O) stretching at 1041.3 cm^{-1}, and δ (Si—O—Al) at 520 cm^{-1} respectively. The absence of 3267 cm^{-1} stretching frequency [Figs. 1(b)–1(d)] of free OH, broadening of 3436 cm^{-1} peak with a shift towards lower frequency and a shift of Si—O stretching vibration towards higher frequency in case of the three nanocomposites prepared with PANI, PMAA, and PANI-*co*-PMAA suggests intercalation of the polymer within clay galleries through OH functional group. Further, the presence of characteristic vibration peaks of PANI and PMAA confirm polymerization of PANI and PMAA as well as PANI-co- PMAA in the bentonite clay layers. Nanocomposites of PANI with MMT, reported by Biswas and Ray[33] did not reveal any shift in the FTIR spectra of the nanocomposites, suggesting the exfoliation of the polymer in the clay, while the same reported by Lee et al.[34] were found to undergo a considerable shift in the CN vibration peaks, thus confirming intercalation of the polymer within the clay galleries.

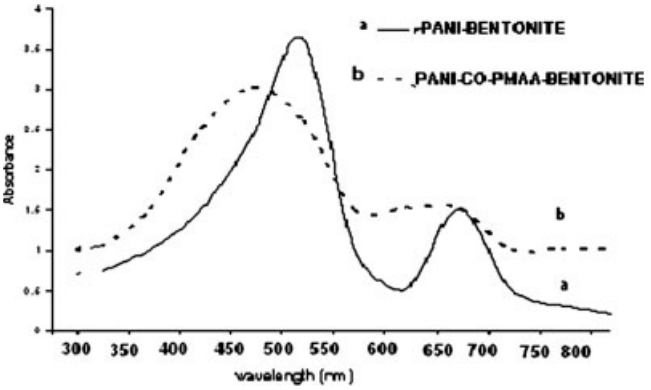

Figure 2 UV–visible spectra of PANI/bentontie and PANI-*co*-PMAA/bentonite.

UV–visible spectra

The UV–visible spectra of PANI-bentonite Figure 2(a) show absorption maximas around 500 and 650 nm. The peak in the UV range at 500 nm can be correlated to Π–Π * transitions in the benzenoid structure whereas the peak in the visible range around 700 nm is related to the doping level of PANI and formation of polarons/bipolarons respectively.[35] The peak values confirm the presence of doped form of PANI, i.e., emeraldine salt forms in bentonite.[35] In case of PANI-*co*-PMAA-bentonite, Figure 2(b), we find that the transitions in the UV range as well as in the visible range appear to be broad and show a

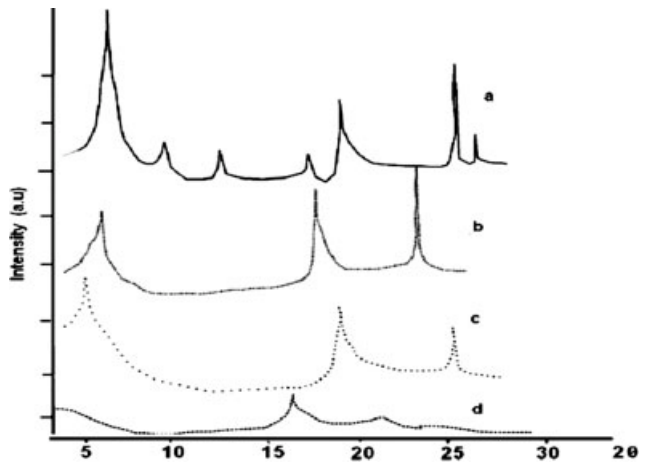

Figure 3 XRD of (a) bentonite, (b) PANI/bentonite, (c) PMAA/bentonite, and (d) PANI-*co*-PMAA/bentonite.

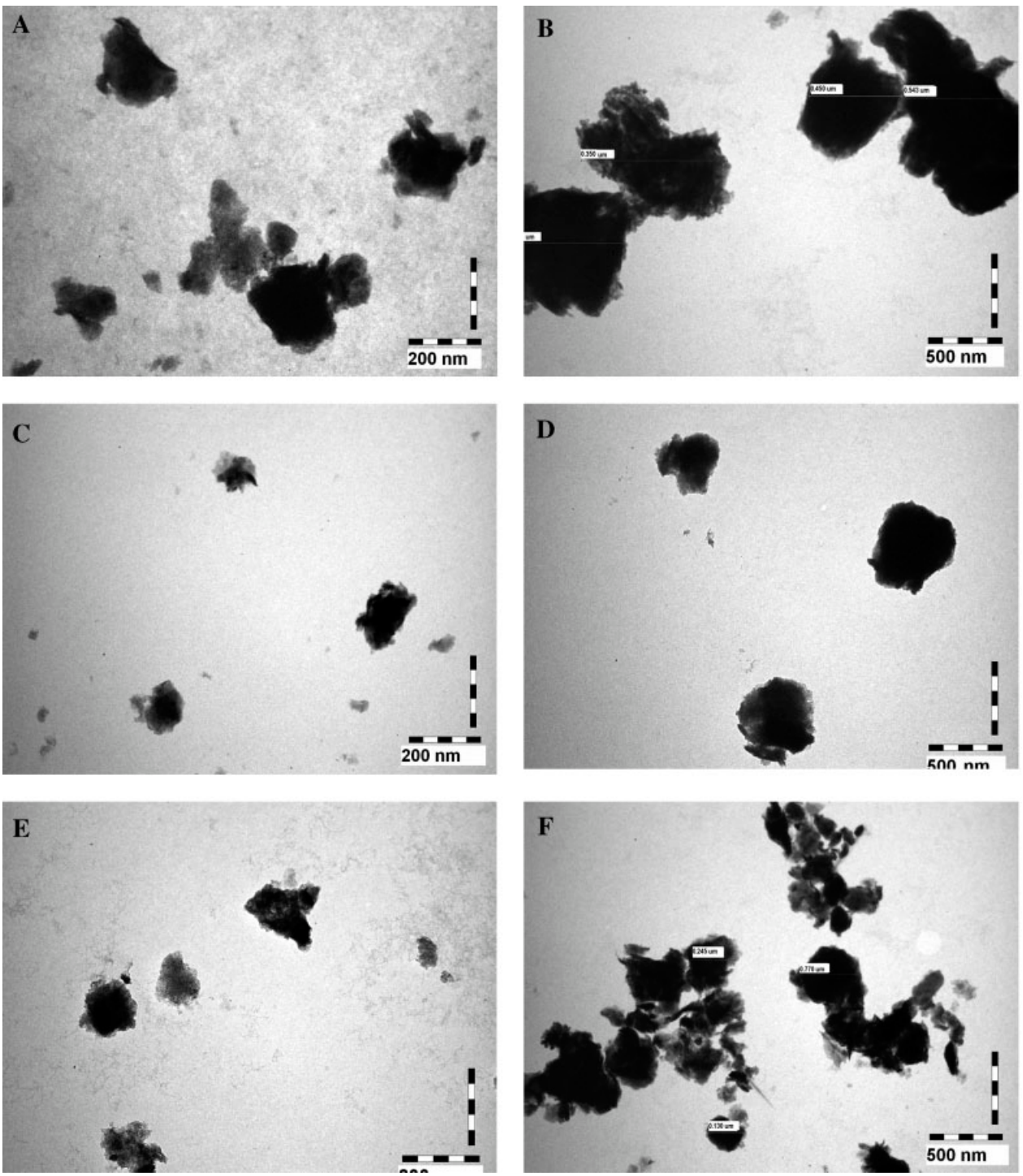

Figure 4 TEM micrograph of (a) PANI/bentonite (200 nm), (b) PANI/bentonite (500 nm), (c) PMAA/bentonite (200 nm), (d) PMAA/bentonite (500 nm), (e) PANI-*co*-PMAA/bentonite (200 nm), and (f) PANI-*co*-PMAA/bentonite (500 nm).

hypsochromic shift which can be attributed to the presence of an extended chain conformation of PANI causing more delocalization of polarons. The polaronic transitions appear larger in case of the copolymer as the peak in the visible range appears to be expanded, indicating higher doping level in this case. Thus, it can be concluded that PANI/bentonite and PANI-*co*-PMAA/bentonite are present in the doped state within the modified bentonite clay.[2]

XRD analysis

The (001) reflection peak of the pristine bentonite is observed around $2\theta \sim 5.7^\circ$ and 7.0° for calcium and

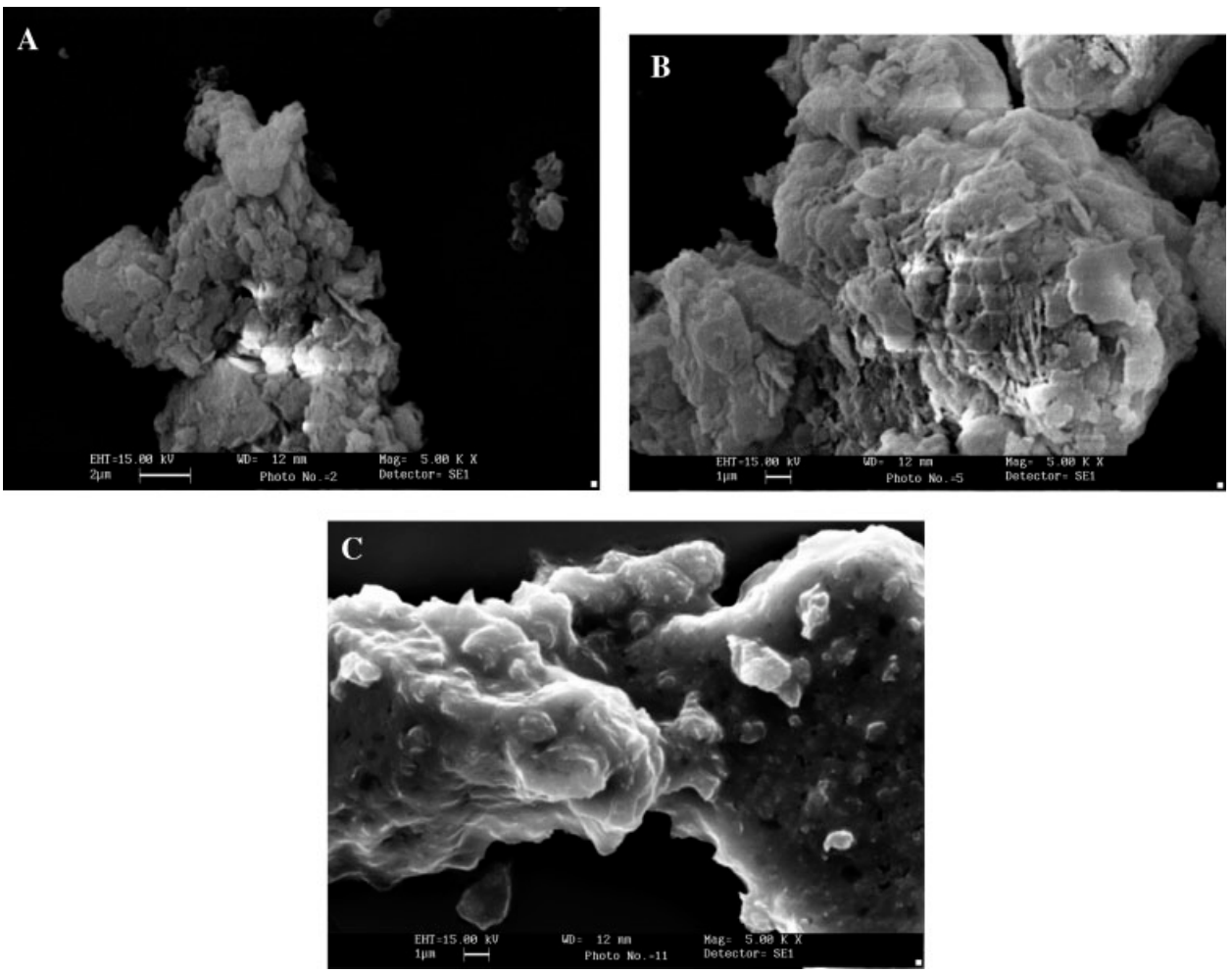

Figure 5 SEM micrograph of (a)PANI/bentonite (×5000), (b) PMAA/bentonite (×5000), (c) PANI-*co*-PMAA/bentonite (×5000).

sodium form respectively [Fig. 3(a)]. In the present case, bentonite shows 100% intensity at $2\theta = 5.9^\circ$, which corresponds to basal spacing of 1.49 nm (calculated using Scherrer equation $2d \sin \theta = n\lambda$). In case of polymer/clay nanocomposites, it is shifted towards lower angles. When compared with bentonite, the diffraction patterns of PANI-bentonite and PMAA-bentonite nanocomposites show a shift of the basal peak position from $d = 1.49$ to 1.69 nm and 1.8 nm respectively. The increase in the *d*-spacing can be attributed to the increase in the gallery height upon intercalation of the polymers in the clay galleries. We find an appreciable increase of 0.2 and 0.30 nm in the interlayer spacing of PANI-bentonite and PMAA-bentonite nanocomposites. The expansion observed in our case is comparable to the ones reported for polyaniline-MMT[34] having similar concentration of monomer in the clay. The observed expansion of the clay gallery reflects relatively high intercalation content probably due to the higher extent of polymerization in the two cases.[8] Biswas and Ray[33] ruled out any intercalation in PANI/MMT composites while Kim et al.[26] have found a basal expansion of 0.34 nm. In the case of the PANI/layered inorganic solid nanocomposites, the interlayer expansion generally varies in the range of 0.3–0.6 nm. However, the PANI-*co*-PMAA/bentonite [Fig. 3(d)] nanocomposite shows absence of characteristic (001) diffraction peak. It can be presumed that the 001 diffraction peak appears to be shifted to still lower values as the conformational transition from a compact coil to an expanded coil leads to significant increase in the height of the gallery and has been reported by Wan and coworkers[36] in case of PANI intercalated in clay particles upon secondary doping. Hence, values at lower angle of 2θ (around $2\theta = 2^\circ$) would have been preferable to establish intercalation as higher inter layer expansion is observed in this case.

It can be concluded that the intergallery expansion of clay layers observed in all the three nanocomposites confirms the successful insertion of polymer as well as copolymer chains between silicate layers.

TEM studies

The TEM micrograph of PANI/bentonite at low magnification [Fig. 4(a)] shows the presence of clusters of PANI-bentonite particles. Interestingly, the bentonite particles are not observed and appear to be encapsulated by PANI clusters. The average diameter of the particles was found to be in the range of 250–350 nm upon higher magnification [Fig. 4(b)]. The TEM micrograph of PMAA/bentonite [Fig. 4(c)] also reveals a nearly granular, nearly spherical morphology of small clusters at low magnification, and the aggregate size is found to be in the range of 250–300 nm upon higher magnification [Fig. 4(d)]. However, the TEM micrograph of PANI-*co*-PMAA/bentonite [Fig. 4(e)] shows huge clusters of varying sizes, some of which are found to be spherical in shape. Higher magnification reveals the agglomerate size of 400–500 nm [Fig. 4(f)]. The formation of large clusters in this case may be attributed to the copolymerization of two monomers in the bentonite layers. Being water-soluble monomers, PANI and PMAA start polymerizing in aqueous medium and the insoluble polymers glue the silica leading to the formation of larger aggregates. In all the nanocomposites no silicate nanolayers are observed, as they appear to be encapsulated by the polymers as well as copolymer.

SEM studies

The SEM micrograph of PANI/bentonite [Fig. 5(a)] shows the presence of granular aggregates, reflecting its layered nature with minute high density granules per unit area. The morphology appears to be uniform and homogeneous, indicating no phase separation, which can be attributed to the intercalation of PANI in bentonite. The SEM micrograph of PMAA/bentonite [Fig. 5(b)] also shows an aggregate granular morphology with clusters of granules present, revealing a more compact and dense structure. The granules are observed to be nearly spherical in nature. However, the SEM of PANI-*co*-PANI bentonite [Fig. 5(c)] shows a mixed morphology with the presence of flaky as well as granular structures.[8]

TG-DTA analysis

In general the first weight loss in bentonite [Fig. 6(a)] just below 100°C is due to the loss of water from interlayer galleries. The second weight loss at 221°C is believed to be due to onset of first decomposition event. The third decomposition event occurs at 620°C, as shown in DTG curve. This weight loss is attributed to the dehydroxylation of silicate structure. In case of PANI/bentonite [Fig. 6(b)] the thermal behavior shows a gradual weight loss, as can be seen from the minima in DTG curve, indicating the majority weight loss for respective steps. The first step weight loss just below 100°C is attributed to the loss of water and the second weight loss at 287°C is assigned to the thermal decomposition of PANI backbone chains.[27] The intercalated nanocomposite is shifted to higher temperature by about 66°C. Only 10 wt % weight loss is observed at 287°C. This suggests that the intercalated nanocomposite is more thermally stable than is pure PANI, as observed by some authors in case of PANI-MMT.[29] The PMAA/bentonite nanocomposite [Fig. 6(c)] shows 10 wt % loss at 278°C, while 30 wt % loss is observed at 426°C, hence the nanocomposite is not as stable as PANI/Bentonite. In case of PANI-*co*-PMAA/bentonite [Fig. 6(d)], the nanocomposite has highest stability and shows 10 wt % loss at 339°C. The thermal stability observed in our case is comparable to the one reported by Biswas and Ray[33] in case of PANI-MMT. From these observations it can be concluded that PANI-*co*-PMAA/bentonite shows overall highest thermal stability.

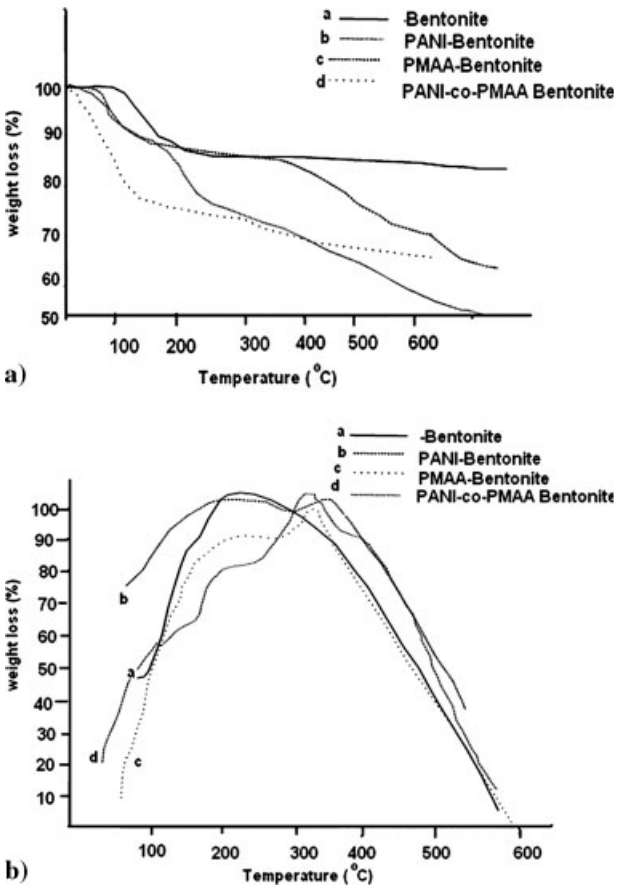

Figure 6 TGA (left panel) and DTA (right panel) of (a) bentonite, (b) PANI/bentonite, (c) PMAA/bentonite, and (d) PANI-*co*-PMAA bentonite.

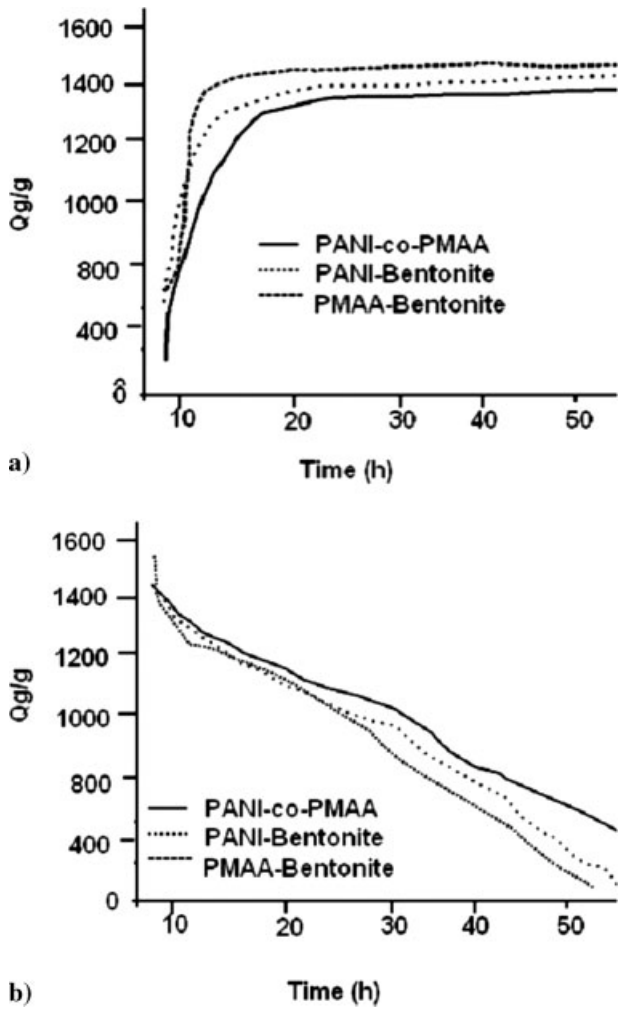

Figure 7 (a) Swelling behavior of PANI/bentonite, PMAA/bentonite and PANI-*co*-PMAA bentonite; (b) degradation behavior of PANI/bentonite, PMAA/bentonite, and PANI-*co*-PMAA bentonite.

Swelling and degradation studies

The results of swelling experiments [Fig. 7(a)] support that silicate can crosslink with PMAA and PANI, and the crosslinking degree increases in a certain range, showing the dynamic water swelling of PANI, PMAA, and PANI-*co*-PMAA nanocomposites within 50 min. Sample without bentonite has no chemical crosslinks in the structure and can dissolve completely within 30 min after being immersed in water whereas PANI/bentonite, PMAA/bentonite, and PANI-*co*-PMAA/bentonite are partly crosslinked and can dissolve completely after several hours. All of the three samples can absorb water by about 1400 times more than its dry weight in 5 min.[3]

The crosslinking structures of the nanocomposites resulted from Si—O—C bonds between PMAA and PANI chains and silicate. For Si—O—C bonds hydrolyzed in aqueous solution, the hybrids tend to degrade in aqueous solution. Figure 7(b) shows the degrading behavior of nanocomposites. After 24 h, lose of weight for PANI/bentonite, PMAA/bentonite, and PANI-*co*-PMAA/bentonite are 45, 37, and 35%, respectively. Forty-eight hours later, the weight loss percentages are 95, 88, and 73%, respectively. It has been observed that although the equilibrium absorbencies of the three samples are close, the degrading rates slow down as the amount of silicate increases, which may result from the increase in the amount of Si—O—Si networks in the system.[37]

CONCLUSIONS

Nanocomposites of bentonite with PANI, PMAA, and their copolymer was successfully synthesized. The PANI/bentonite as well as PANI-*co*-PMAA/bentonite were found to exhibit intercalation while exfoliation was observed in case of PMAA/bentonite. PANI-*co*-PMAA/bentonite nanocomposite was found to show highest stability with 10 wt % loss at 339°C. The equilibrium absorbencies of the three nanocomposites were found to be close and the degrading rates slowed down as the amount of silicate increased. The swelling behavior suggests that these nanocomposites can be used as effective chemical absorbents of impurities (such as toxic solvents and dyes) commonly found in waste water. Studies on the absorption of dyes by these nanocomposites are in progress in our laboratory and will be published soon.

References

1. Theng, B. K. G. The Chemistry of Clay-Organic Reactions; Wiley: New York, 1974.
2. Ogawa, M.; Kuroda, K. Bull Chem Soc Jpn 1997, 70, 2593.
3. Kojima, Y.; Usuki, A.; Kawasumi, M.; Okada, A.; Fukushima, Y.; Karauchi, T.; Kamigaito, O. J Mater Res 1993, 6, 1185.
4. Lerner, M.; Oriakhi, C. In Handbook of Nanophase Materials; Goldstein, A., Ed.; Marcel Dekker: New York, 1997; p 199.
5. Lagaly, G. Introduction: From clay mineral/polymer interactions to clay mineral/polymer nanocomposites. Appl Clay Sci 1999, 15, 1.
6. Greenland, D. J. J Colloid Sci 1963, 18, 647.
7. Ogata, N.; Kawakage, S.; Ogihara, T. J Appl Polym Sci 1997, 66, 573.
8. Billingham, J.; Breen, C.; Yarwood, J. Vib Spectrosc 1997, 14, 19.
9. Usuki, A.; Kojima, Y.; Kawasumi, M.; Okada, A.; Fukushima, Y.; Kurauchi, T.; Kamigaito, O. J Mater Res 1993, 8, 1179.
10. Usuki, A.; Kawasumi, M.; Kojima, Y.; Okada, A.; Krauchi, T.; Kamigaito, O. J Mater Res 1993, 8, 1174.
11. Kojima, Y.; Usuki, A.; Kawasumi, M.; Okada, A.; Kurauchi, T.; Kamigaito, O. J Polym Sci Part A: Polym Chem 1993, 31, 983.
12. Vaia, R. A.; Giannelis, E. P. Macromolecules 1997, 30, 7990.
13. Vaia, R. A.; Giannelis, E. P. Macromolecules 1997, 30, 8000.
14. Liu, L. M.; Qi, Z. N.; Zhu, X. G. J Appl Polym Sci 1999, 71, 1133.
15. Carrado, K. A.; Xu, L. Q. Chem Mater 1998, 10, 1440.
16. Yang, Y.; Zhu, Z. K.; Yin, J.; Wang, X.Y.; Qi, Z. E. Polymer 1999, 40, 4407.

17. Gilman, J. W.; Jackson, C. L.; Morgan, A. B.; Harris, R., Jr.; Manias, E.; Giannelis, E. P.; Wuthernow, M.; Hilton, D.; Phillips, S. H. Chem Mater 2000, 12, 1866.
18. Lepoittevin, B.; Devalckenaere, M.; Pantoustier, N.; Alexandre, M.; Kubies, D.; Calberg, C.; Jerome, R.; Dubois, P. Polymer 2000, 43, 1111.
19. Yasmin, A.; Jandro, L. A.; Isaac, M. D. Scripta Mater 2003, 49, 81.
20. Chen-Yang, Y. W.; Yang, H. C.; Li, G. J.; Li, Y. K. J Polym Res 2004, 11, 275.
21. Straw, H. K. E.; Manias, E. Chem Mater 2000, 12, 2943.
22. Hasegawa, N.; Kawasumi, M.; Kato, M.; Usuki, A.; Okada, A. J Appl Polym Sci 1998, 67, 87.
23. Yoon, J. T.; Jo, W. H.; Lee, M. S.; Ko, M. B. Polymer 2001, 42, 329.
24. Li, P.; Tan, T. C.; Lee, J. Y. Synth Met 1997, 88, 237.
25. Joo, J.; Song, H. G.; Jeong, C. K.; Beack, J. S.; Lee, J. K. Synth Met 1999, 98, 215.
26. Kim, B. H.; Jung, J. H.; Joo, J.; Epstein, A. J.; Mizoguchi, K.; Kim, J. W.; Choi, H. J. Macromolecules 2002, 35, 1419.
27. Wu, Q.; Xue, Z.; Qi, Z.; Wang, F. Polymer 2029, 41 2000.
28. Yang, S. M.; Chen, K. H.; Synth Met 2003, 135, 51.
29. Yoshimoto, S.; Ohashi, F.; Kanneyama, T. Macromol Rapid Commun 2004, 25, 1687.
30. Tong, X.; Zhao, H.; Tang, T.; Feng, Z.; Huang, B. J Polym Sci Part A: Polym Chem 2003, 40, 1706.
31. Forte, C.; Geppi, M.; Giamberini, S.; Ruggeri, G.; Veracini, C. A.; Mendez, B. Polymer 1998, 39, 2651.
32. Gao, D.; Heimann, R. B.; Williams, M. C.; Wardhaugh, L. T.; Muhammad, M. J Mater Sci 1999, 34, 1543.
33. Biswas, M.; Ray, S. S. J Appl Polym Sci 2000, 77, 2948.
34. Lee, D.; Lee, S. H.; Char, K.; Kim, J. Macromol Rapid Commun 2000, 21, 1136.
35. Monkman, A. P. In Conjugated polymeric Materials; Bredas, J. L., Chance, R. R., Eds.; Kluwer: Dordrecht, The Netherlands, 1990. NATO ASI Series E: Applied Sciences, Vol. 182, p 273.
36. Dai, L.; Wang, Q.; Wan, M. J Mater Sci 2000, 19, 1645.
37. Ye, H.; Zhao, J.; Zhang, Y. J Appl Polym Sci 2004, 91, 936.